For editor Gerrit Lohmann,

What follows is a short letter addressing the changes made in the revised manuscript. Then a marked-up manuscript is attached.

We have changed the title in order to better represent the new version, which now includes a discussion of the mechanism of variability, in addition to the global impacts.
The new hosed-unhosed simulation provides a much better test of the effect of freshwater, by using the same large freshwater flux as the other experiments. The results have been reworded in order to properly convey the new, clearer results. Additionally, we have taken advantage of newer results from the unhosed simulation, which allow us to compare hosed and unhosed experiments directly (i.e. without normalization to an AMOC decrease). All figures have been updated accordingly.

As requested by anonymous reviewers, 3 new figures were added to the main text. First, 2 new figures (one in main text and one in SI) now clearly demonstrate the mechanism of oscillation in the unhosed simulation. Rewriting of the associated text now provides many more details and references. Second, one new figure explains the context of the unhosed simulation within the whole matrix of simulations that we have run with this model. Third, since sea ice extent and winter mixed-layer depth were important to our arguments, we have followed the proposition of an anonymous reviewer and added one figure depicting the geographical extent of sea ice and mixed-layer depth.

As requested by the editor, the southern ocean freshening is explored in greater detail both in the text and in a new supplementary figure.

Every single major and minor comment from anonymous reviewers has translated into respective modifications of the revised manuscript.

If you have found any of the mentioned changes to be ambiguous, do not hesitate to contact us for clarification.

Sincerely,
Nicolas Brown and Eric Galbraith

Manuscript prepared for Clim. Past
with version 2015/04/24 7.83 Copernicus papers of the LaTeX class copernicus.cls.
Date: 18 March 2016

# Hosed vs. Unhosed: ~~Global response to~~ interruptions of the Atlantic Meridional Overturning in a global coupled model, with and without freshwater forcing

Nicolas Brown[1] and Eric D. Galbraith[1,2,3]

[1]Dept. of Earth and Planetary Science, McGill University, Montreal QC H3A 2A7
[2]Institucio Catalana de Recerca i Estudis Avanats (ICREA), 08010 Barcelona, Spain
[3]Institut de Ciencia i Tecnologia Ambientals (ICTA) and Department of Mathematics, Universitat Autonoma de Barcelona, 08193 Barcelona, Spain

*Correspondence to:* eric.d.galbraith@gmail.com

**Abstract.** It is well known that glacial periods were punctuated by abrupt climate changes, with large impacts on air temperature, precipitation, and ocean circulation across the globe. However, the long-held idea that freshwater forcing, caused by massive iceberg discharges, was the driving force behind these changes has been questioned in recent years. This throws into doubt the abundant literature on modelling abrupt climate change through 'hosing' experiments, whereby the Atlantic Meridional Overturning Circulation (AMOC) is interrupted by an injection of freshwater to the North Atlantic: if some, or all, abrupt climate change was not driven by freshwater input, could its character have been very different than the typical hosed experiments? Here, we ~~take advantage of a global coupled ocean-atmosphere model that exhibits~~ describe spontaneous, unhosed oscillations in AMOC strength ~~, in~~ that occur in a global coupled ocean-atmosphere model when integrated within a particular envelope of boundary conditions. We compare these unhosed oscillations to hosed oscillations under a range of boundary conditions in order to examine how the global imprint of AMOC variations depends on whether or not it is the result of external freshwater input. ~~The results imply that , to first order , the ocean-ice-atmosphere~~ Our comparison includes surface air temperature, precipitation, dissolved oxygen concentrations in the intermediate-depth ocean, and marine export production. The results show that the background climate state has a significant impact on the character of AMOC interruptions, including marked variations in tropical precipitation and in the North Pacific circulation. Despite these differences, the first order response to AMOC interruptions is quite consistent among all simulations, implying that the ocean-sea ice-atmosphere dynamics associated with an AMOC weakening dominate the global response, regardless of whether or not freshwater input is the cause. ~~The exception lies in the~~ Notable exceptions lie in the direct impact freshwater inputs can have on the strength of other polar haloclines, particularly the Southern Ocean, to which freshwater can be transported relatively quickly after injection in the North Atlantic.

## 1 Introduction

'Abrupt' climate changes were initially identified as decadal-centennial temperature changes in Greenland ice deposited during the last ice age (?) , and subsequently recognized as globally-coherent climate shifts (??). Abrupt climate changes were shown to have involved changes in the latitudinal extent and strength of the AMOC (?), but also impacted global patterns of precipitation, surface air temperature, ocean biogeochemistry and atmospheric trace gas composition ~~(???)~~ (??????) . Abrupt climate changes were associated, ~~early on, with dramatic~~ in early studies, with layers of ice-rafted detritus that blanketed the North Atlantic during brief intervals of the last ice age (?), leading to the idea that recurring pulses of freshwater input had been the cause of AMOC interruptions. As evocatively described by ?, armadas of icebergs, periodically discharged from the northern ice sheets to melt across the North Atlantic (?), would have spread a freshwater cap that impeded convection and consequently, through the ? feedback, would have thrown a wrench in the overturning. Inspired by this idea, generations of numerical models have been subjected to freshwater 'hosing' experiments, whereby the sensitivity of the AMOC to varying degrees of freshwater input have been ~~plumbed~~tested, and the responses shown to vary as a function of background climate state and experimental design ~~(??????????)~~ (????????????) . Multiple studies have shown a good degree of consistency between aspects of these hosing simulations and the observed global signatures of abrupt climate change ~~(??)~~ (???) .

However, other model simulations have shown that spontaneous changes in the AMOC can occur in the absence of freshwater inputs ~~(????????????)~~ (??????????????) . Although uncommon, these 'unhosed' ~~simulations~~ oscillations show that the AMOC can vary as a result of processes internal to the ocean-atmosphere system, ~~most importantly through the existence of multiple stable~~ which have been linked to oscillations in the strength of the vertical density gradient in the North Atlantic (???) , and to the existence of unstable states of the sea ice extent in the North Atlantic (????). In addition, there are features of the observational records that are inconsistent with iceberg armadas having been the driving force behind all episodes of abrupt climate change (?). Periods of ~~rapid~~ abrupt Greenland cooling are typically divided between 'Heinrich events', for which widespread ice-rafted detritus is found (?), and 'Dansgaard-Oeschger stadials' (?), which include all abrupt Greenland coolings, but are not associated with widespread ice rafted detritus. In Greenland ice core records, Heinrich events are very similar to Dansgaard-Oeschger stadials, despite the apparent contrast in the associated amount of ice rafted detritus and, presumably, the consequent freshwater input.

What's more, the arrival of ice-rafted detritus does not seem to precede changes in the AMOC, where the two are recorded together. An analysis of Heinrich event 2 in the NW Atlantic showed that weakening of the AMOC preceded the widespread deposition of ice-rafted detritus by approximately 2 ky (?), while a statistical analysis of the temporal relationship between ice-rafted detritus near Iceland and dozens of cold events in Greenland suggested that ice-rafted detritus deposition generally lags the onset of cooling by a significant amount (?). These observations throw further

doubt on the role of iceberg melting as the universal driver of abrupt climate change. In fact, it may be more likely that iceberg release is more often a consequence of AMOC interruptions, rather than necessarily being their cause, ~~as~~ a possibility raised by the identifications of subsurface warming during AMOC interruptions in hosed model simulations (**?**). Such intermediate-depth warming of the North Atlantic, resulting from the reduced release of oceanic heat at high latitudes, would have melted floating ice shelves at their bases, contributing to ice sheet collapse (**????**). Thus, although there is good evidence that large iceberg armadas were released during ~~some~~ most stadials, and would have freshened the North Atlantic accordingly, they were not necessarily the main causal factor involved in all stadials. This raises the question: does the global footprint of an AMOC interruption depend on its cause, or is any AMOC interruption the same, regardless of whether or not freshwater forcing was behind it? How does the importance of the causal driver compare with the sensitivity to the background climate state, itself determined by $CO_2$, terrestrial ice sheets, and the Earth's orbital parameters?

In order to explore these questions, we make use of a large number of long water-hosing simulations with CM2Mc, a state-of-the-art Earth System model, to show how the global response to hosing varies between a preindustrial and glacial background state, and under different orbital forcings. In addition, we take advantage of the fact that the same model exhibits previously undescribed spontaneous AMOC interruptions and resumptions, which appear very similar to stadial-interstadial variability, to reveal what aspects of the abrupt changes are a result of the hosing itself rather than consequences of the changing AMOC.

## 2 Experimental Setup

### 2.1 Model Description

The simulations shown here use the coupled ocean-atmosphere model CM2Mc, as described in **?**. This is a moderately low resolution, but full complexity model, that includes an atmospheric model that is at the high-complexity end of the spectrum applied in previously-published water hosing simulations. In brief, the model includes: a 3-degree finite volume atmospheric model, similar to ~~that~~ the 2-degree version used in the GFDL CM2.1 ~~model (?)~~ (**?**) and ESM2M (**?**) models; MOM5, a non-Bousinnesq ocean model with a fully-nonlinear equation of state, subgridscale parameterizations for mesoscale and submesoscale turbulence, vertical mixing with the KPP scheme as well as due to the interaction of tidal waves with rough topography but otherwise a very low background vertical diffusivitity (0.1 $cm^2\ s^{-1}$), similar to that used in the GFDL ESM2M model (**?**); a sea-ice module, static land module, and a coupler to exchange fluxes between the components. In addition, the ocean model includes the BLING biogeochemical model as described in **?**. This includes limitation of phytoplankton growth by iron, light, temperature and phosphate, as well as a parameterization of ecosystem structure.

### 2.2 Experimental Design

The ~~ten~~ experiments shown here vary in terms of the prescribed atmospheric $CO_2$, the size of terrestrial ice sheets, and the Earth's orbital configuration (obliquity and precession). Terrestrial ice sheets were set to either the 'preindustrial' extents, or the full LGM reconstruction of the Paleoclimate Model Intercomparison Project 3 (https://pmip3.lsce.ipsl.fr), in which case the ocean bathymetry was also altered to represent lowered sea level, including a closed Bering Strait, and ocean salinity was increased by 1 PSU. Atmospheric $CO_2$ concentration has a value of either 270 or 180 ppm depending on whether the ice sheets have a preindustrial or glacial extent, respectively. The obliquity was set to either 22.0°or 24.5°, spanning the calculated range of the last 5 My (**?**). The precessional phase, defined as the angle between the Earth's position during the northern hemisphere autumnal equinox and the perihelion, was set to two opposite positions, corresponding to the positions at which the boreal seasonalities are least and most severe (90°and 270°, respectively). All other boundary conditions of the model were configured as described in **?**.

Freshwater forcing ('hosing') was applied to four simulations run under 'Preindustrial' conditions with ~~extrema~~ the four possible combinations of obliquity and precession~~values, and another~~ , and a corresponding four under 'Glacial' conditions~~also with extrema obliquity and precession~~. For each of these eight hosing simulations, the model was initialized from a previous preindustrial or LGM state, run for 1000 years, a freshwater hosing was applied for 1000 years, and then it was run for a further 1000 years with the hosing off. Control simulations (without hosing) were also run for the same length of time as the hosing to allow drift correction. During hosing, freshwater was added in the North Atlantic by overriding the land-to-ocean ice calving flux with a preindustrial annual mean plus an additional 0.2 Sv evenly distributed in a rectangle bounded by 40N to 60N and 60W to 12W. Because the same preindustrial mean background calving flux was used in all hosings, for the five non-preindustrial hosings, this also represents a 0.018 Sv increase in the calving flux on the Antarctic coast relative to the background glacial climate. It should be noted that because the model does not have a rigid lid, this represents a 'real' freshwater input to the ocean. The result is a global sea level rise of ~~15~~ 17 m over the 1000 year hosing, representing approximately one third the ~~rate of sea level rise estimated for the~~ maximum rate of sea level rise estimated during the last deglaciation (Melt Water Pulse 1a) (**?**). For the top panels of Figures ~~2-7~~5-10, the 'weak' AMOC state is defined as years 901-1000 of hosing, and the 'strong' AMOC state is the same century taken from the corresponding control simulation to correct for drift, which was quite small.

In addition, we show results from a simulation for which hosing was not applied, but which exhibits spontaneous oscillations in the AMOC reminiscent of D-O events~~, very similar to those of ?~~. This 'Unhosed' simulation was conducted under glacial $CO_2$ (180 ppm), but with preindustrial ice sheets and bathymetry, low obliquity, and weak boreal seasonality. The Unhosed simulation was one of a suite of simulations integrated with constant forcing, under the same simultaneous changes in obliquity, precession and ice sheet configuration described above but under a broader

range of $CO_2$ variations (Galbraith et al., in prep). The strength of the AMOC varies considerably among these simulations, with stronger AMOC occurring at high $CO_2$ and with full glacial ice sheets (Figure 1), for reasons that will be discussed elsewhere (Galbraith et al., in prep). Strikingly, two of the simulations (those with 180 ppm $CO_2$, low obliquity, and preindustrial ice sheets) were found to show oscillations between two unstable states of the AMOC, reminiscent of D-O changes (Figure 1). Of these, the simulation with weak boreal seasonality gradually settled into longer oscillations with a period of ~1200 yrs, closer to the period of the observed D-O cycles, after a few millennia of more rapid oscillations. Given the greater similarity to the period of observed D-O cycles, this simulation is taken as the 'Unhosed' example. In this Unhosed simulation, the weak AMOC state is defined by averaging the last century of an 'unforced' AMOC decrease (model years 7501-7600) and the strong AMOC state is defined by averaging a century following an 'unforced' AMOC increase (model years 7901-8000).

The final experiment is a modification of the Unhosed simulation, in which ~~a small (0.05 Sv ) hosing is applied~~ the 0.2 Sv hosing perturbation is applied to the North Atlantic during a strong-AMOC interval. This final experiment provides an explicit test of the effect of a hosed vs. an unhosed AMOC weakening.

## 3 Results

### 3.1 Simulated changes in the North Atlantic

The eight hosed simulations show a number of common features in the North Atlantic, which vary as a function of boundary conditions (Figure ~~1~~2). Within the first two centuries of hosing, the Greenland temperature rapidly drops by 8-15 °C, with a stronger response under high obliquity. When the hosing is stopped, the temperatures abruptly increase by 8-20 °C, again with a stronger response under high obliquity, and under glacial conditions. ~~The~~ Overall, the simulated magnitudes of warming and cooling are of the same magnitude as reconstructed for abrupt climate change from Greenland ice cores (**?**). The AMOC follows a very similar temporal progression in all cases, which is the inverse of the sea ice extent in the North Atlantic. The average North Atlantic sea surface salinity drops by 2-4 PSU in the hosed simulations, consistent with the generally-accepted mechanism of a halocline strengthening due to freshwater forcing, associated with an expansion of sea ice, being the cause of an AMOC interruption. Thus, as shown by many prior simulations, the hosing response is quite consistent with observations and the idea of iceberg armadas shutting down the AMOC and initiating abrupt climate change (**??**).

However, Figure ~~1~~ 2 also shows the same metrics of North Atlantic variability for the Unhosed simulation. Under the low $CO_2$, low obliquity and preindustrial ice-sheets of this simulation, the model's coupled ocean-atmosphere system ~~adopts a mode of circulation whereby the AMOC spontaneously oscillates between 12-15~~ causes the AMOC to spontaneously oscillate between 15-18 Sv and 6 Sv,

on a centennial timescale (Figures ~~1,~~ 2, 3). Although the amplitude of the variations in the Unhosed simulation tends to be smaller than in the hosed simulations, with a weaker AMOC throughout (Figure ~~2), and the timescale of fluctuations tends to be shorter than the imposed forcing of the Hosed simulations, the~~ 3), the general relationship between the four variables is quite similar (Figure ~~1).~~ 2). When AMOC is weak, North Atlantic deep convection is greatly reduced and shifted to the south, while sea ice expands in the northeast Atlantic, in both the hosed and Unhosed simulations (Figure 4). Thus, the Unhosed oscillations are also consistent with observational evidence that a strengthened halocline, associated with an expansion of sea ice, were coupled to a weakening of the AMOC - even in the absence of external freshwater forcing. ~~A very similar type of~~ This variability follows in the long tradition of spontaneous AMOC oscillations observed among simpler models, and appears to be very similar to the unforced AMOC oscillation ~~was~~ observed recently in the Community Earth System (CESM) model, which is of similar complexity but run at higher resolution, by **?**.

The ~~Unhosed variability in CM2Mc can be understood as follows. While the AMOC is weak~~ spontaneous millennial AMOC oscillations that occur in ocean circulation models can generally be described as 'deep decoupling oscillations' (**?**) . These oscillations include a weak overturning phase, during which convection is reduced and/or shifted to lower latitudes (**?**) , allowing the deep polar ocean to accumulate heat, ~~heat accumulates in the subsurface North Atlantic (500 m-1500 m) due to the northward transport of heatfrom the low latitude thermocline, while the strong halocline impedes the downward mixing of cold surface waters. Eventually, the temperature inversion that results from the buildup of heat at depth counteracts the halocline to the point at which the water columncan be destabilized. In the model this occurs when a high-salinity anomaly at the sea surface , caused by decadal variability in precipitation andevaporation, as observed in the modern ocean (?) , triggers open-ocean convection. Following destratification, the AMOC rapidly accelerates to its strong state within five years, while the rapid release of heat from the warm subsurface waters melts back the North Atlantic sea-ice area by as much as 80 . The summer sea iceretreat has a large impact on the local radiative balance by changing albedo, while the winter sea ice retreat allows much more sensible and latent heat release to the atmosphere, so that the Greenland annual average temperature jumps by 10 °C within a decade. Over the next decades to centuries, the strong-AMOC state gradually decays back to a state with greater North Atlantic sea-ice, a low AMOC of 6 Sv and cold Greenland temperatures~~transported northwards by diffusion at depth. The accumulation of heat gradually destabilizes the polar water column, until deep convection resumes in a 'thermohaline flush' (**?**) . The reinvigorated overturning carries salty subtropical waters north, further strengthening the overturning (**??**) . A gradual decrease of the poleward surface temperature gradient (**?**) and/or salinity gradient (**?**) causes a gradual weakening of the overturning, until some point at which the AMOC weakens nonlinearly and the weak phase returns. It has been suggested that expansions of sea ice, which tend to amplify the polar halocline by exporting brines to depth and building up fresh

layers due to melt at the surface, could have been key to stratifying the northern North Atlantic and driving the AMOC into its weak mode (**???**) .

The ~~coupled ocean-ice-atmospheric oscillations exhibited by~~ changes in AMOC, sea ice and surface salinity in the Unhosed simulation ~~are quite consistent with the mechanism proposed by **?** , using a simple box model, as well as by **?** based on observations from the Nordic seas~~(Figure 2) are consistent with this general scenario. It is remarkable that the magnitude of the salinity change in the unforced simulations is on the order of more than 1 PSU, nearly half as much as for the hosing simulation under the same $CO_2$ and orbital configuration (Figure ~~1~~2), in spite of the absence of any external sources of freshwater, and a reduction of precipitation relative to evaporation over the North Atlantic. The surface freshening is therefore caused by the changes in ocean circulation and sea ice cycling. Figure 5 shows that, during the weak AMOC phase, heat accumulates at depth in the North Atlantic due to the northward diffusion of warm waters from the tropics and lack of flushing by cold North Atlantic Deep Water (**?**) . At the same time, the salinity increases at the tropical Atlantic surface (**?**) , and the poleward surface temperature gradient intensifies (**?**) . Paleoceanographic reconstructions from D-O events are consistent with both the accumulation of tropical sea surface salinity (**?**) and the simulated changes in water column temperature and salinity in the Nordic seas (**?**) . The buildup of heat at intermediate depths in the subpolar North Atlantic helps to weaken the stratification (Supplementary Figure 7), so that it can be overcome when a saline surface anomaly disrupts the halocline, triggering deep convection. Given that changes in temperature have a significant role, in addition to changes in salinity, it would appear most appropriate to call the mechanism in the Unhosed simulation a 'thermohaline oscillator', rather than the simpler 'salt oscillator' described by (**?**) . ~~In accordance with the suggestion of **???** , and the similar simulation of **?** , we propose that this type of nonlinear changes in sea ice extent, and their coupling with the oceanic and atmospheric circulation, are at the essence of abrupt climate change.~~

Next, we show how the global consequences of changes in the AMOC depend on the background climate state, and the question of whether or not they are forced by freshwater addition. We do so by exploring a few key atmospheric and oceanic variables that have well-documented responses to abrupt climate change as recorded by paleoclimate records.

### 3.2 Global atmospheric response

Abrupt climate change was initially identified in ice core proxy records of atmospheric temperature, and subsequently extended to temperature variations recorded in multiple proxies from around the world (**?**). Figure ~~3~~ 6 summarizes the global surface air temperature change that occurs in response to our simulated AMOC interruptions. ~~Note that, because the AMOC changes vary significantly between the simulations, all anomalies are normalized to an AMOC change of 10 Sv in Figures 3-7.~~ The first order patterns of surface air temperature change are very similar between the preindustrial and glacial boundary conditions, as well as in the unhosed simulation. The northern hemisphere un-

dergoes general cooling in the extratropics, with greatest cooling in the North Atlantic from Iceland to Iberia, and with cooling extending into the tropics of the ~~eastern~~ North Atlantic, North Africa, and southeast Asia. ~~The region of maximum cooling in the Pacific occurs at the Kuroshio-Oyashio confluence, consistent with a southward shift in the front.~~ Meanwhile, the southern hemisphere warms everywhere except in the western tropical Pacific and Indian oceans. The maximum warming occurs at high latitudes of the Southern Ocean, and is associated with a sea ice retreat (Figure 5). The general temperature pattern is consistent with the idea of a bipolar seesaw (**??**).

One notable difference in the spatial patterns is the temperature change in the ~~NE~~ N Pacific, including the western margin of Canada and southern Alaska. The temperature here is quite sensitive to the degree of northward transport of warm ocean water from the subtropical gyre, which is quite variable between simulations. All ~~preindustrial~~ hosed simulations develop a ~~strong~~ Pacific Meridional Overturning Circulation (PMOC) when the AMOC weakens, previously described in models as an Atlantic-Pacific Seesaw (**?????**). The ~~development of~~ degree to which a PMOC develops varies substantially between simulations, with stronger development of PMOC in the preindustrial hosings. The development of a strong PMOC counteracts the hemisphere-wide cooling in the NE Pacific, which can actually cause a warming. This suggests that temperature proxy records from this region would provide strong observational constraints on the degree to which a PMOC developed during abrupt climate changes. The simulations that develop a strong PMOC also show a region of maximum cooling at the Kuroshio-Oyashio confluence, consistent with a southward shift in the front.

The strength of the bipolar seesaw also varies significantly as a function of background climate state, due to differences in both the southern hemisphere and the North Atlantic. Stronger southern warming occurs under glacial conditions, and with the combination of high obliquity and strong boreal seasons (Supplementary Figure 2). The temperature response to hosing in the North Atlantic is particularly dependant on orbital configurations in glacial simulations because of different initial sea-ice extents which are strongly driven by obliquity (~~standard deviation in Figure~~ Figure 2, 3~~and Supplementary Figure 1). Otherwise, the response in glacial and preindustrial conditions is fairly consistent between the four extrema orbital configurations~~rd row, compare initial sea ice area under glacial and preindustrial).

In general, the temperature response in the Unhosed simulation is very similar to the ensemble means of the hosed simulations, and would appear to have a relatively weak southern warming. The weak southern warming is partly due to the fact that southern warmings develop slowly, and the time between the Unhosed 'stadial' and 'interstadial' is relatively short (~400 yrs). If the 'interstadial' reference years are taken at the end of an interstadial, rather then the middle, a stronger southern warming, more similar to that of preindustrial hosed simulations, is observed (Supplementary Figure 8). The spatial differences between the Unhosed and the hosed simulations are generally of the same order as the differences among the hosed simulations under different background states.

Changes in precipitation during abrupt climate changes have also been well-documented in speleothems and marine sediment records (???) . As shown in Figure 47, the overall patterns of change are similar between Hosed hosed and Unhosed simulations, as they were for the changes in temperature, including reduced precipitation in . The robust, common patterns include reduced precipitation over the North Atlantic, a southward shift of the Intertropical Convergence Zone (ITCZ), previously shown to be a direct result of the sea ice expansion associated with stadials (?) , and reduced precipitation over south Asia.

In fact, many aspects of the precipitation changes vary more as a function of background climate state, including orbital configuration, than they do between Hosed and Unhosed . The hosed and Unhosed (Supplementary Figure 3). Thus, not only is the mean state of tropical precipitation sensitive to orbital forcing (?) , but the response of tropical precipitation to an AMOC disruption is sensitive to orbital forcing as well. Perhaps the two most notable differences between among the simulations are the pattern of change surrounding the west Pacific warm pool, an extremely dynamic region with heavy precipitation, and the NE Pacific and western North America, where changes in precipitation follow the sea surface temperature through its control on water moisture content and atmospheric circulation. The response to hosing in the region surrounding the west Pacific warm poolis an area whose response to hosing is , including Indonesia and NE Australia, is strongly dependant on orbital configuration (standard deviation in Figure 4), mostly precession (Supplementary Figure 2). 3). For example, with weak boreal seasons, hosing tends to cause an increase in precipitation north of Borneo, which does not occur when boreal seasons are strong.

### 3.3 Global ocean biogeochemistry response

The observed footprint of abrupt climate change also extends to ocean biogeochemistry, with pronounced and well-documented changes in both dissolved oxygen concentrations and export production. Prior work has shown that many aspects of the observed oxygenation changes (**?**) and export production changes (**??**) can be well reproduced by coupled ocean-biogeochemistry models under hosing experiments.

As shown by Figure 58, our model simulations produce consistent changes in intermediate-depth oxygen during AMOC weakening, hosed or unhosed, that agree well with the bipolar seesaw-mode changes in oxygenation extracted from sediment proxy records of the last deglaciation by ? (?) . All simulations show a decrease of oxygen throughout the full depth of the North Atlantic, due to the lack of ventilated North Atlantic Deep Water, and an increase in the oxygenation of the intermediate-depth North Pacific and Arabian Sea. We note that the North Pacific changes reveal a pronounced shift in the southeastward penetration of North Pacific Intermediate Water, with a hotspot of oxygen change where the edge of the strongly-ventilated thermocline impinges on the California margin. This hotspot implies that a tendency for a frontal shift to occur in this region makes it particularly

sensitive to changes in the AMOC, and explains why the California borderlands region has such rich records of oxygenation changes on millennial timescales (???) .

~~As shown by Figure 6, the simulated changes in the North Pacific and Arabian Sea are driven by large changes in ventilation, that overcome basin-wide changes in export production (Figure 7) acting in the opposite direction (i.e. greater export when intermediate-depth oxygen is higher). The primary discrepancies between the simulations are in the degree of oxygen enrichment in the subarctic Pacific, again related to the development of a PMOC, the changes in ventilation in the Tropical Atlantic thermocline, and in the degree of ventilation changes in the Southern Ocean.~~

The relative changes in export production, shown in Figure ~~7~~9, are locally quite large (in excess of 100%) but have weaker regional patterns that are less consistent between simulations. The most consistent strong features are a reduction of export in the northern North Atlantic, the western tropical North Atlantic, and the southern margin of the Indo-Pacific subtropical gyre, and an increase in export off of NW Africa, to the west of California, and in the high latitude Southern Ocean. Regions that do not always respond consistently are the subarctic Pacific, which depends significantly on whether or not a PMOC develops, and the Pakistani margin~~and eastern tropical Pacific, which both show~~ , which shows an increase in export under ~~hosing as observed by ? except under glacial hosing, when they do not change.~~ pre-industrial, but not glacial hosing. It is important to point out that, because the model does not resolve coastal upwellings, it is probably missing important changes. This may explain, for example, the fact that decreases in primary production are not simulated on the Baja California margin during hosings, as reconstructed during stadials (?) . In general, the differences between the various hosed simulations is as large as the difference between hosed and unhosed.

The simulated changes of export production show an overall decrease globally, consistent with prior results (???) , which contributes to the simulated increase of intermediate-depth oxygen concentrations during stadials by reducing oxygen consumption. In addition, oxygen supply to intermediate depths of the northern Indo-Pacific is increased by more rapid flushing of thermocline waters during stadials, indicated by lower ventilation ages (Figure 10), also consistent with other models (?) . The primary discrepancies in intermediate-depth age between the simulations are in the subarctic Pacific, again related to the development of a PMOC, changes in ventilation in the Tropical Atlantic thermocline, and in the degree of ventilation changes in the Southern Ocean.

### 3.4 Hosing the Unhosed

The analyses above suggest that most of the large-scale responses of climate and ocean biogeochemistry to an AMOC disruption are ~~quite~~ similar regardless of whether the interruption is forced through hosing or as a spontaneous result of internal model dynamics. In order to further test this apparent insensitivity ~~of results to the trigger~~ to the cause of AMOC weakening, we applied a freshwater forcing during a strong AMOC interval of the Unhosed simulation, forcing the model to return to

~~its~~ a weak AMOC state earlier than in the standard Unhosed case. This experiment provides a direct comparison between an unforced and a freshwater forced AMOC reduction. The freshwater forcing weakens the AMOC transport (Figure ~~1~~2, black line in 3rd column), and maintains its weakened state over the full 1000 year simulation, whereas the Unhosed simulation ~~returned~~ returns to the strong-AMOC state after about 800 years. By comparing both the forced and unforced simulations after 800 years of stadial, we can estimate the differences caused by the freshwater itself~~(Figure 8)~~.

~~As shown, the~~ The changes caused by ~~freshwater itself are quite small compared to the overall changes (compare Figure 8 with Figures 3-7 and Supplementary Figures 1-4). Surface air temperatures only differ significantly~~ the freshwater addition are shown in Figure 11, which can be compared with the Unhosed variability in Figures 6, 7, 8, and 9. The change in surface air temperatures differs little as a result of the hosing, with significant contrasts only in the North Atlantic, North Pacific, and high latitude Southern Ocean~~, while precipitation and oxygen generally show~~ . Precipitation shows a much larger response under hosing, which is generally an amplification of the Unhosed trends, ~~and~~ though the impact over western Indonesia is a uniformly strong drying rather than the mixed response of the Unhosed case. Dissolved oxygen also shows an amplification of the Unhosed trends when hosed, though the changes are relatively small, while export production shows ~~minimal changes except for~~ changes mainly in the N Atlantic and NE Pacific. ~~Most of these differences~~ The general amplification of changes can be understood by the fact that the freshwater-forced simulation has a ~~slightly~~ weaker AMOC, and more extensive North Atlantic sea-ice coverage, leading to ~~slightly~~ lower temperatures in the NE Atlantic and a correspondingly greater response in atmospheric circulation that amplifies most features of the weak-AMOC state.

The fact that precipitation responds most strongly suggests that, among the metrics examined here, it has the greatest sensitivity to the intensification of the Unhosed stadial by hosing, which could reflect a fairly direct link between the northern sea ice edge and/or North Atlantic cooling, latitudinal sea surface temperature gradients, and the Hadley circulation (**??**) . Essentially, a stronger push from the northern extratropics leads to a stronger response in the tropical hydrological cycle. Observations showing that precipitation responses were markedly different during Heinrich stadials as opposed to non-Heinrich stadials in Borneo (**?**) , northeastern Brazil (**?**) and the Cariaco basin (**?**) are therefore consistent with Heinrich stadials representing much stronger interruptions of the AMOC (**?**) , that led to greater sea ice expansion and North Atlantic cooling, and consequently larger shifts in tropical precipitation.

Apart from the ~~small~~ amplification of the general trends, we note one distinct additional feature: the ~~Antarctic temperature response~~ southern hemisphere warming is decreased under hosing, weakening the bipolar seesaw. This feature of the Antarctic response appears to reflect the transport of freshwater from the North Atlantic to the Southern Ocean~~through relatively shallow pathways in the Atlantic~~, in addition to the small increase in calving flux from the Antarctic margin (Supplementary Figure 9), so that ~~it freshens~~ the Southern Ocean surface is freshened. The addition of freshwater

strengthens the Southern Ocean halocline, reducing ocean heat release and keeping a larger mantle of sea ice around Antarctica. Thus, the cooler Southern Ocean does not reflect a different response to the AMOC weakening itself, but rather a secondary effect of the freshwater addition through its direct influence on the vertical density structure of the Southern Ocean. We note that **?** found an opposite effect of freshwater input on the Southern Ocean, with a relative weakening of the halocline causing a destratification of the Southern Ocean under freshwater forcing. It would thus appear that this aspect of hosing is quite sensitive to model behaviour and experimental design. Given the potential importance of Southern Ocean convection on ~~controlling~~ modifying atmospheric $CO_2$ ~~(**???**) , this is not a trivial finding~~(**????**) , careful consideration should be made of freshwater input to the Southern Ocean derived from the melting of local Antarctic (**??**) or distant northern hemisphere ice sheets.

## 4 Discussion and conclusions

Our Unhosed model simulation adds to a small, but growing subset of complex 3-dimensional ocean-atmosphere model simulations exhibiting unforced oscillations similar to the abrupt climate changes of Dansgaard-Oeschger cycles. Under a particular set of boundary conditions (low $CO_2$, with preindustrial ice sheets and low obliquity), it ~~can spontaneously switch to a much weaker state~~spontaneously oscillates between strong and weak AMOC states, triggered by internal climate variability within the model, acting on a type of '~~salt~~ thermohaline oscillator'. ~~This model behavior is essentially identical to that described by **?** and **?** .~~

~~These~~ The Unhosed simulation was integrated under perfectly stable boundary conditions, with no variability in external factors such as solar output, aerosols or freshwater runoff. Such additional variability might make it easier for spontaneous AMOC variations ~~suggest that when~~ to occur in reality, as long as the AMOC is in relatively a weak state due to the background climate state, ~~it is easy for it to switch into an off mode with very little forcing. Under these conditions~~leading to AMOC oscillations under a wider range of background conditions. Thus, large volcanic eruptions (**?**), ice-sheet topography changes (**?**) or ~~ocean-atmosphere climate variability controlling precipitation in the North Atlantic, would be sufficient to~~ solar variability could all potentially trigger an abrupt change ~~. However, the ubiquitous~~ in the real world, without requiring freshwater input, even when the climate system is in a more stable mode than that of the Unhosed simulation. Nonetheless, the fact that weakening of the AMOC ~~that~~ always occurs in models under sufficient hosing implies that, even in a strong mode, the AMOC is vulnerable to freshwater forcing, if it is large enough.

As previously suggested, melting of ~~ice shelves~~ floating ice shelves due to subsurface ocean warming could provide an important feedback to an initial AMOC weakening, accelerating ice sheet mass loss due to their buttressing-effect on upstream ice, and adding freshwater that would ~~help stabilize the AMOC in a~~ push the AMOC into a very weak mode (**???**). Such a behaviour is similar

to that exhibited here by the Hosed-Unhosed simulation, and may have been necessary to produce a complete 'shutdown' of the AMOC, as suggested by Pa/Th measurements at Bermuda Rise (**?**). This suggests that the question of whether or not a Heinrich event occurred during an AMOC interruption had more to do with the susceptibility of the Laurentide ice sheet to collapse than the nature of the initial AMOC interruption itself. In turn, the degree to which consequent ice sheet melting altered ocean circulation may have depended on where the freshwater was discharged, including how much of the freshwater was input to the ocean as sediment-laden hyperpycnal flows (**??**).

Although they only occur in our model under an unrealistic combination of boundary conditions, ~~a fact which is likely sensitive to the parameterization of deep ocean mixing (?) , the~~ the spontaneous nature of these oscillations allows a powerful comparison to be made with the more typical freshwater-hosed simulations of AMOC weakening. When compared with the Hosed simulations, the general features of the atmospheric and oceanic responses are remarkably robust, with climate background state playing as great a role in determining the response as whether the AMOC weakening was spontaneous or forced. These robust features can therefore be taken to reflect consistent dynamical changes related to the AMOC interruption and its coupling with sea ice and atmospheric changes, independent of the ultimate cause of the AMOC interruption. ~~The only substantial difference noted~~ Of the variables examined here, tropical precipitation showed the strongest sensitivity to an intensification of AMOC interruption with additional hosing.

An important difference between Hosed and Unhosed simulations lay in the direct impact of freshwater on ocean density structure. ~~The injection of freshwater in the North Atlantic can quickly spread throughout the global ocean, dependent on the distribution of its input and the ocean circulation pattern~~Polar haloclines are very sensitive to freshwater input, which can stratify or destratify them depending on the depth at which freshwater is injected. In our simulations, ~~the most~~ an important consequence of this is the stratification of the Southern Ocean, which ~~is intensified by the freshwater initially injected to the North Atlantic~~could have important consequences for atmospheric $CO_2$. Aside from this ~~relatively minor~~ contrast, the global features of an AMOC weakening appear to depend just as much on the background climate state as they do on its fundamental cause.

*Acknowledgements.* We thank the Canadian Foundation for Innovation (CFI) and an allocation to the Scinet supercomputing facility (University of Toronto), made through Compute Canada, for providing the computational resources. We are ~~also grateful towards the open-source communities behind the development of all the python libraries used to create the graphics for this article, particularly Matplotlib (?) and Cartopy (?)~~ grateful to Olivier Arzel, two anonymous reviewers, and editor Gerrit Lohmann for constructive comments that greatly improved the manuscript.

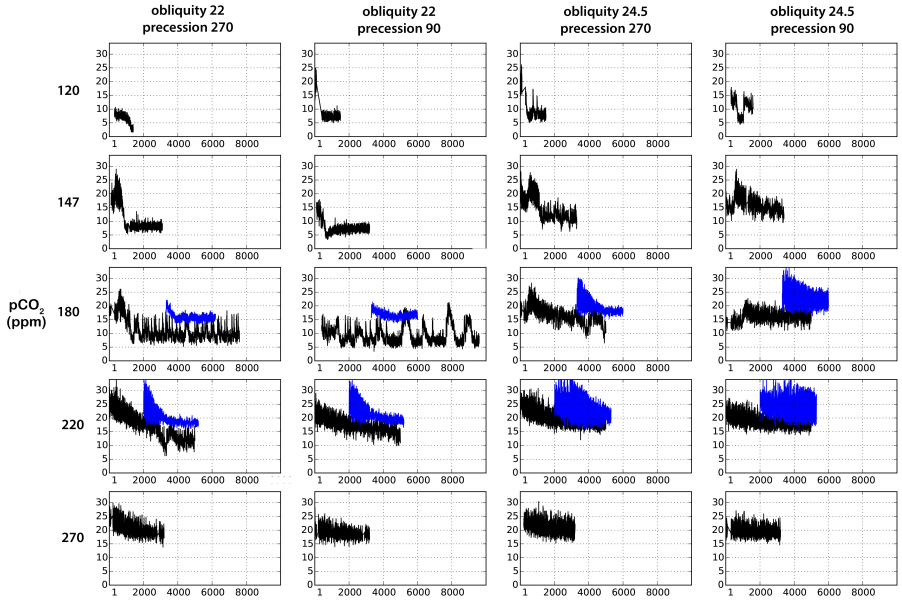


**Figure 1.** Timeseries of AMOC for the matrix of simulations with prescribed atmospheric $pCO_2$ (rows) and orbital configurations (columns). Black lines have preindustrial ice-sheets and blue lines, when applicable, have full LGM ice-sheets. The AMOC, shown on the vertical axes in Sverdrups, is defined as maximum of Atlantic meridional stream function between 30N:50N and water depths of 500:5000m. Precessional phases of 270°and 90°are equivalent to strong and weak boreal seasonalities, respectively.

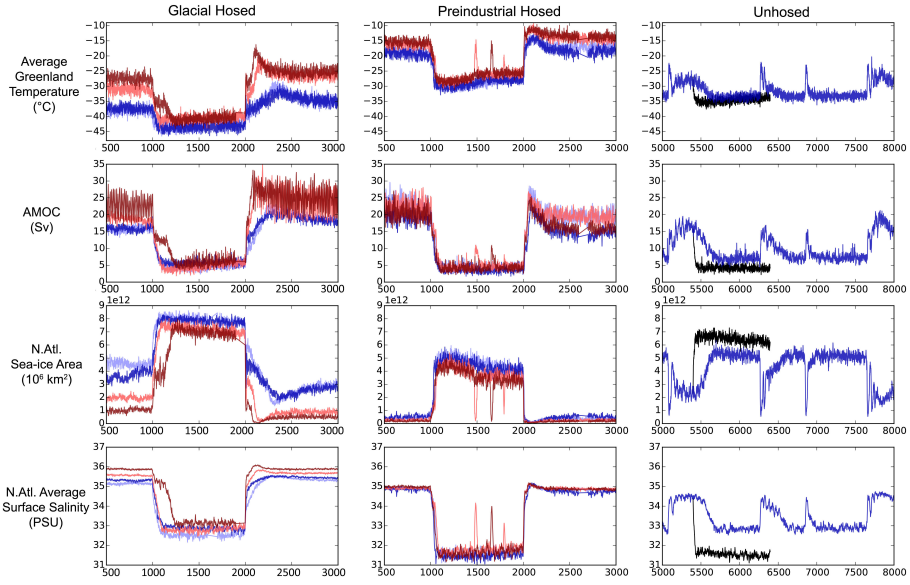


**Figure 2.** North Atlantic climate metrics for all simulations. The left column shows four simulations under the Glacial boundary conditions (LGM ice sheets and bathymetry with closed Bering Strait; 180 ppm $CO_2$), the central column shows four simulations run under the Preindustrial boundary conditions (Preindustrial ice sheets and bathymetry; 270 ppm $CO_2$), and the right column shows the Unhosed simulation in which spontaneous AMOC variations occur under constant boundary conditions. For the left and center columns, freshwater hosing was applied between years 1001 and 2000. Orbital configurations are indicated as follows: red=high obliquity; blue=low obliquity; dark=weak boreal seasonality; pale=strong boreal seasonality. The ~~dark grey~~ black lines in the right column show the 'Hosed-Unhosed' simulation, in which ~~0.05~~ 0.2 Sv of freshwater was added in the North Atlantic during an unforced AMOC 'interstadial'. AMOC is defined as the maximum Atlantic streamfunction between 500m-5500m and 30N:50N.

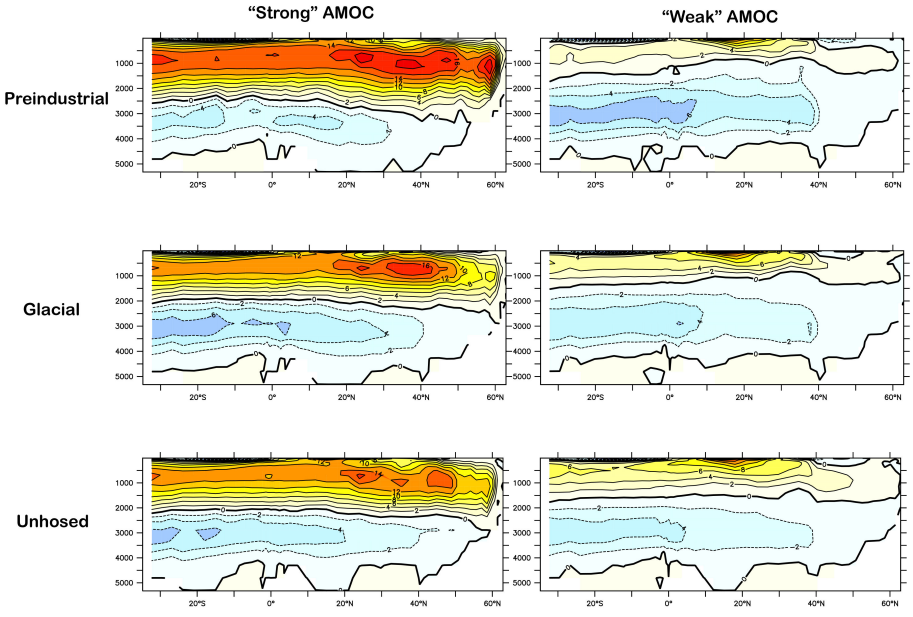


**Figure 3.** Atlantic meridional overturning streamfunctions in strong and weak states. All plots show 100-year averages. In Glacial and Preindustrial hosing simulations, weak AMOC state is defined by averaging the last century of hosing (model years 1901-2000) and strong AMOC state is defined by averaging the same years from the corresponding control simulation (to correct for potential drift). In the Unhosed simulation, the weak AMOC state is defined by averaging model years 7501-7600 and the strong AMOC state is defined by averaging model years 7901-8000. For the top two rows, the streamfunctions are averaged over the corresponding four sets of orbital configurations. The bottom row shows the streamfunctions for the Unhosed simulation. Contours in Sverdrups.

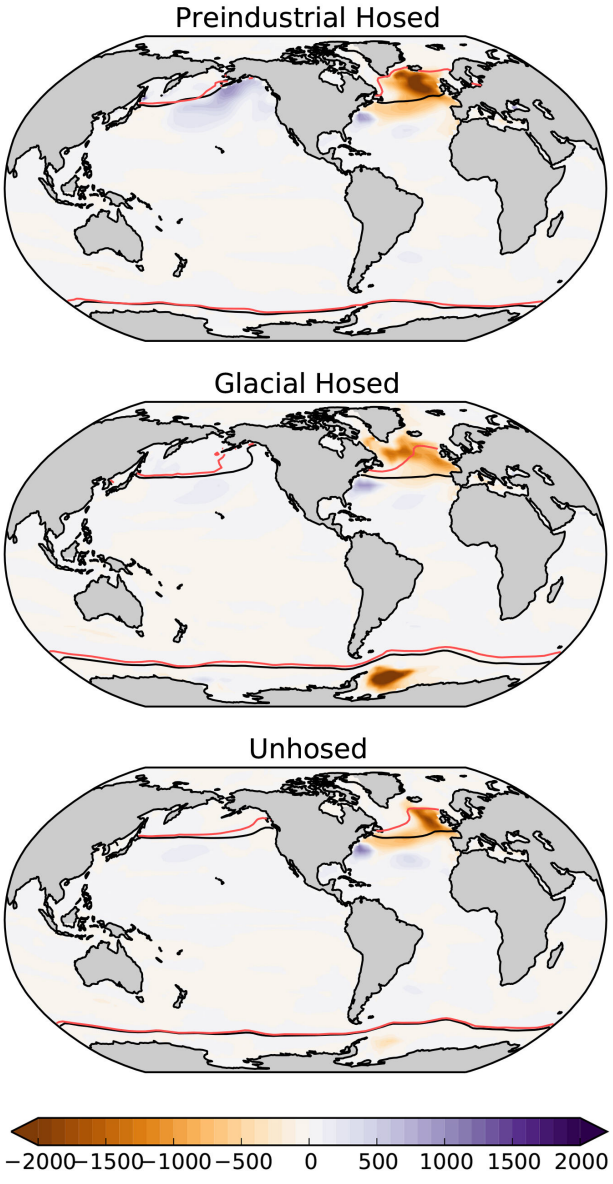


**Figure 4.** ~~Atlantic meridional overturning streamfunctions in strong and weak states~~Stadial winter mixed-layer depth anomaly. ~~All plots~~ The top two panels show ~~100-year averages. In Glacial and Preindustrial hosing simulations, weak AMOC state is defined by averaging~~ the ~~last century of hosing (model years 1901-2000)~~ difference in winter mixed-layer depth between weak and strong AMOC ~~state is defined by averaging the same years from the corresponding control simulation~~ states (~~to correct for potential drift). In the Unhosed simulation, weak AMOC state is~~ as defined ~~by averaging the last century of an 'unforced' AMOC decrease (model years 4981-5080~~in Fig.3) under Preindustrial and ~~strong AMOC state is defined by averaging a century following an 'unforced' AMOC increase (model years 3801-3980). For the top two rows~~Glacial boundary conditions, ~~the streamfunctions are~~ averaged ~~over~~ between the ~~corresponding~~ four sets of orbital configurations (see Supplementary Figure 1 to view all 8 hosing simulations individually). The bottom ~~row~~ panel shows the ~~streamfunctions for~~ winter mixed-layer depth between weak and strong AMOC states (as defined in Fig.3) in the Unhosed simulation. ~~Contours~~ Black and red contours show the sea-ice edge for the weak AMOC and strong AMOC states, respectively. Sea-ice edge is defined as ≥30% of annually-averaged ice concentration. Shading in ~~Sverdrups~~m.

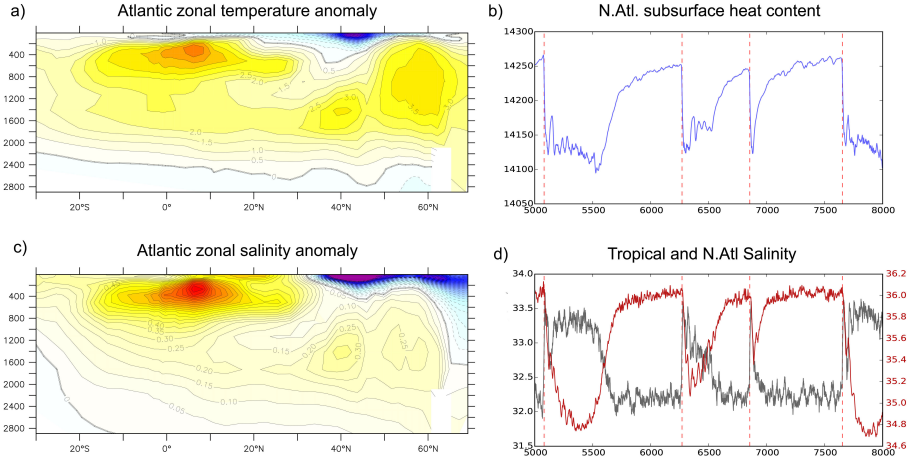


**Figure 5.** Thermohaline oscillations in the Unhosed simulation. a,c) Atlantic zonally-averaged temperature/salinity anomaly between weak AMOC (years 7501-7600) state and strong AMOC state (years 7901-8000). Units in °C / PSU. b) Subsurface (500-2500m) heat content in the North Atlantic (>45°N). Units in ZettaJoules. d) Sea surface salinity in the North Atlantic (>45°N) (black) and Tropical Atlantic (0:10 °N, 70:30 °W) (red). Units in PSU. Red vertical dashed lines indicate onset of deep convection in the North Atlantic.

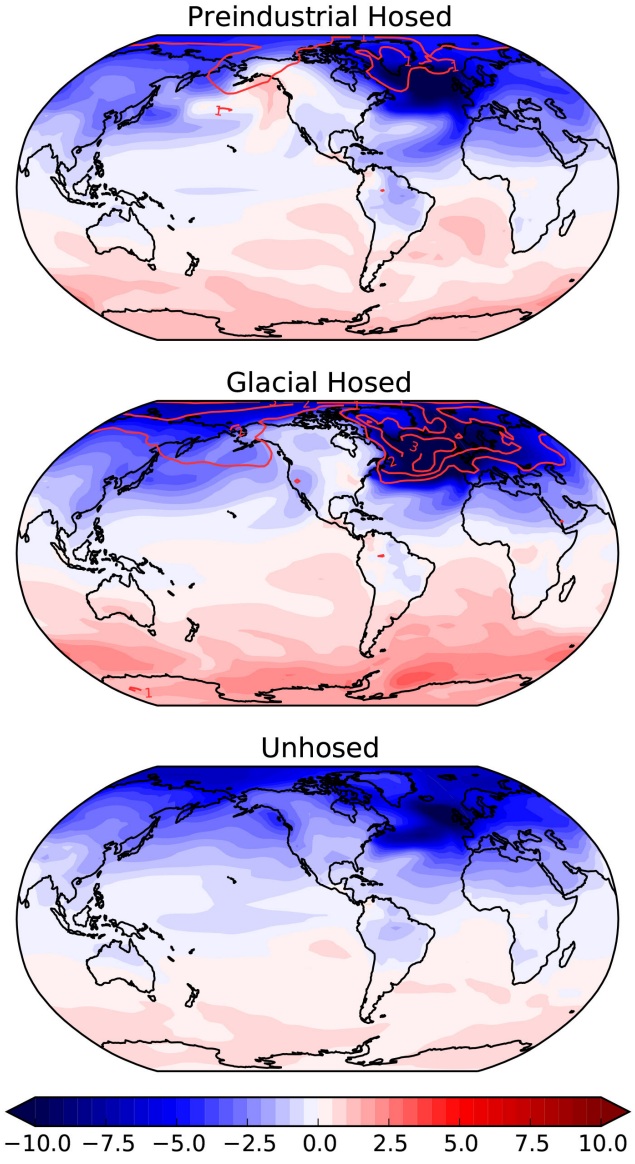


**Figure 6.** Stadial surface air temperature ~~change normalized to a 10 Sv AMOC decrease~~anomaly. The top two panels show the ~~normalized~~ surface air temperature difference between weak and strong AMOC states (as defined in Fig. ~~2~~3) under Preindustrial and Glacial boundary conditions, averaged between the four sets of orbital configurations (see Supplementary Figure ~~1~~ 2 to view all 8 hosing simulations individually). ~~Light grey~~ Red contours show the standard deviation between the four sets of orbital configurations at 1°C intervals. The bottom panel shows the ~~normalized~~ surface air temperature difference between weak and strong AMOC states (as defined in Fig. ~~2~~3) in the Unhosed simulation. Shading and contours in °C.

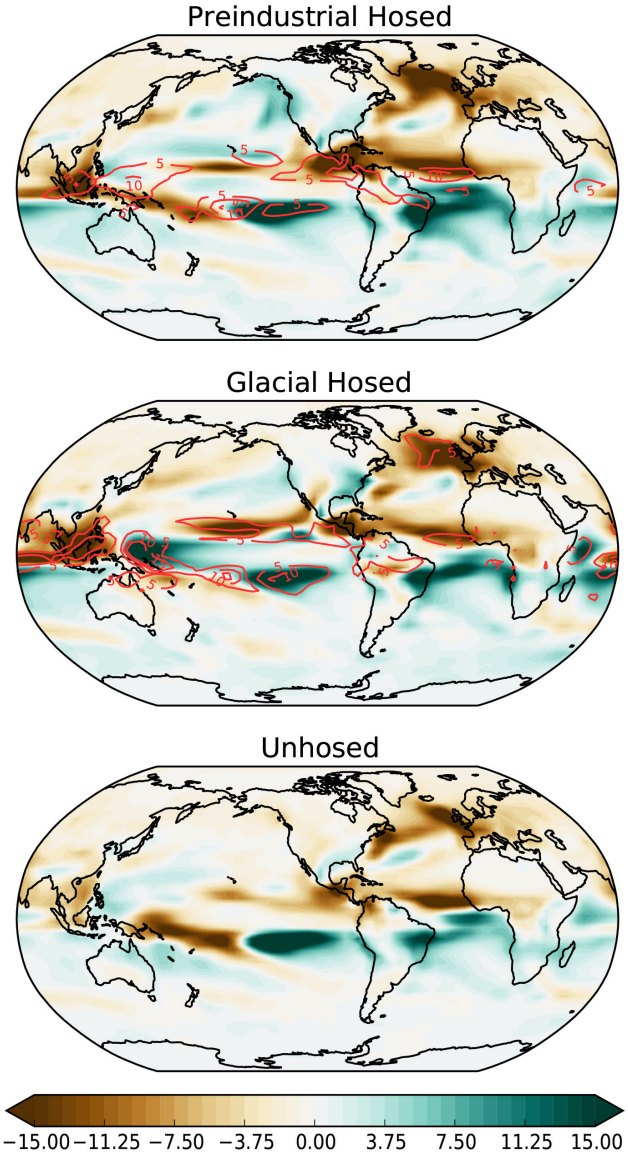


**Figure 7.** Stadial precipitation ~~change normalized to a 10 Sv AMOC decrease~~anomaly. The top two panels show the ~~normalized~~ precipitation difference between weak and strong AMOC states (as defined in Fig. ~~2~~ 3) under Preindustrial and Glacial boundary conditions, averaged between the four sets of orbital configurations (see Supplementary Figure ~~2~~ 3 to view all 8 hosing simulations individually). ~~Grey~~ Red contours show the standard deviation between the four sets of orbital configurations at 5 x $10^{-6}$ kg $m^{-2}$ $s^{-1}$ intervals. The bottom panel shows the ~~normalized~~ precipitation difference between weak and strong AMOC states (as defined in Fig. ~~2~~ 3) in the Unhosed simulation. Shading and contours in $10^{-6}$ kg $m^{-2}$ $s^{-1}$.

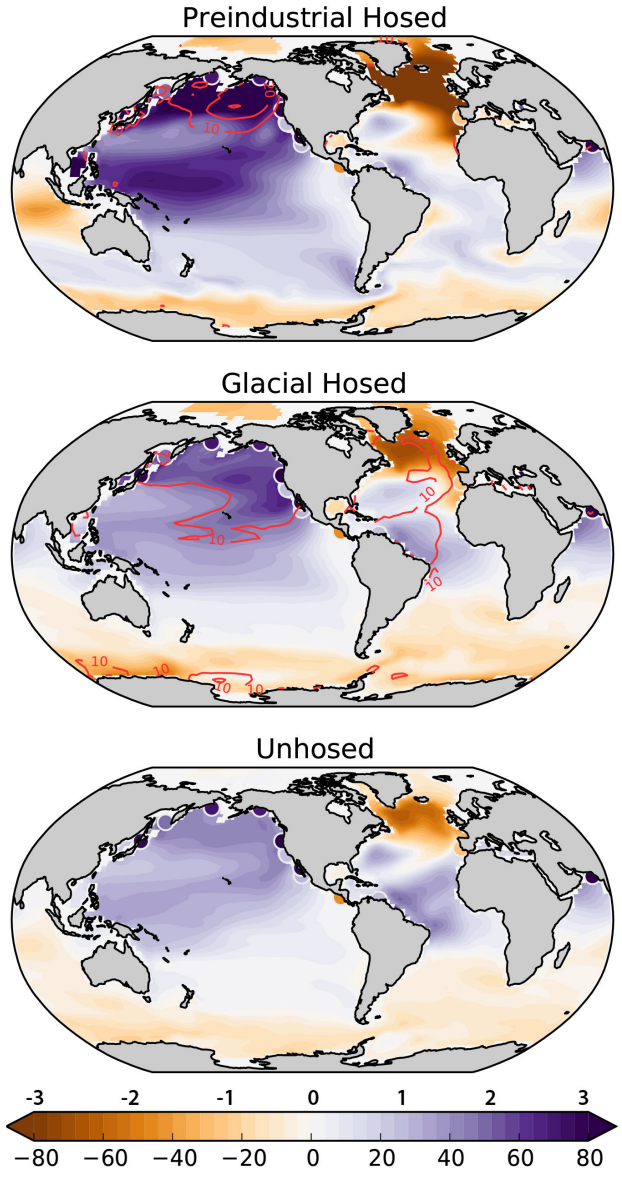


**Figure 8.** Stadial intermediate-depth (~~400m-1400m~~400m-1100m) oxygen concentration ~~change normalized to a 10 Sv AMOC decrease~~anomaly. The top two panels show the ~~normalized~~ oxygen concentration difference between weak and strong AMOC states (as defined in Fig. ~~2~~3) under Preindustrial and Glacial boundary conditions, averaged between the four sets of orbital configurations (see Supplementary Figure ~~3~~ 4 to view all 8 hosing simulations individually). ~~Light grey~~ Red contours show the standard deviation between the four sets of orbital configurations at ~~10 x $10^{-6}$~~ $\mu$mol $kg^{-1}$ intervals. The bottom panel shows the ~~normalized~~ oxygen concentration difference between weak and strong AMOC states (as defined in Fig. ~~2~~3) in the Unhosed simulation. Markers represent the 1st principal component of the detrended time series for benthic oxygenation proxies compiled by **?**. Shading and contours in ~~$10^{-6}$~~ $\mu$mol $kg^{-1}$.

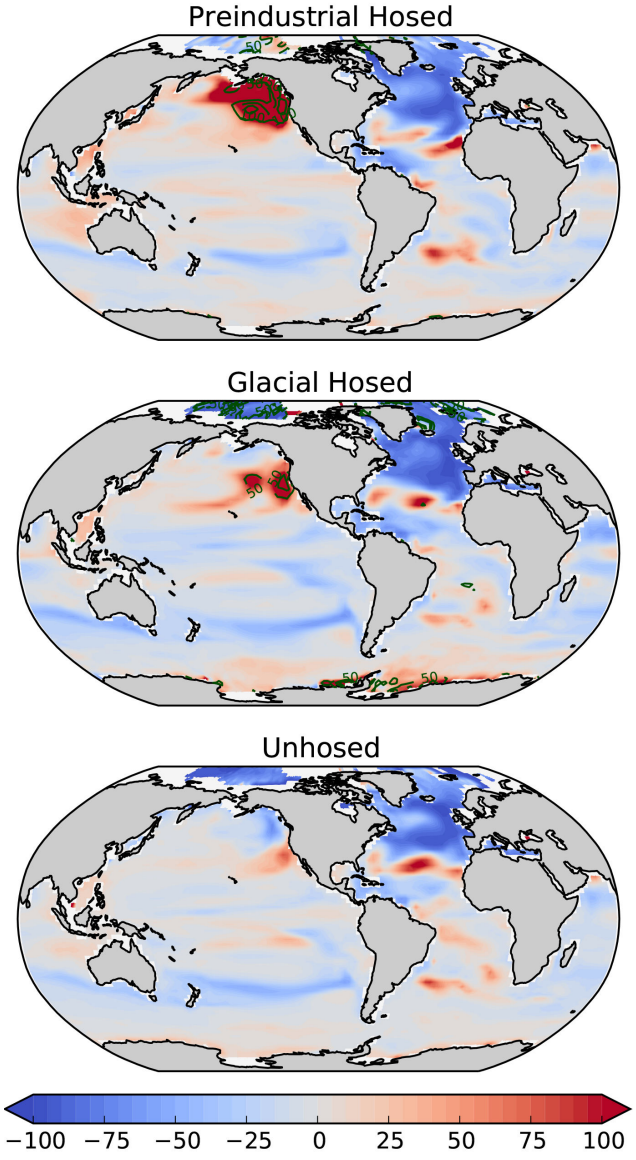


**Figure 9.** Stadial ~~intermediate-depth (400m-1400m) ideal age change normalized to a 10 Sv AMOC decrease~~export production anomaly. The top two panels show the ~~normalized age difference~~ ratio of organic matter export at 100m between weak and strong AMOC states (as defined in Fig. ~~2~~3) under Preindustrial and Glacial boundary conditions, averaged between the four sets of orbital configurations (see Supplementary Figure 5 to view all 8 hosing simulations individually). ~~Light grey~~ Green contours show the standard deviation between the four sets of orbital configurations at ~~30 year~~ 50 % intervals. The bottom panel shows the ~~normalized age difference~~ ratio of export between weak and strong AMOC states (as defined in Fig. ~~2~~3) in the Unhosed simulation. Shading and contours in ~~years~~%.